Unfaulting mechanism of trapped self-interstitial atom clusters in bcc Fe: A kinetic study based on the potential energy landscape

Yue Fan, Akihiro Kushima, and Bilge Yildiz*
Department of Nuclear Science and Engineering, Massachusetts Institute of Technology, 77 Massachusetts Avenue, Cambridge, Massachusetts 02139, USA

(Received 20 November 2009; revised manuscript received 24 January 2010; published 9 March 2010)

We report on the complete unfaulting mechanism of a trapped self-interstitial atom cluster in the form of a nonparallel configuration (NPC), investigated using the autonomous basin climbing (ABC) method. A detailed set of transition state atomic trajectories in the unfaulting process from the trapped to the mobile glide ⟨111⟩ configuration and the corresponding potential energy landscape were identified. The breaking of the initial ring structure of the three trimers on (111) planes followed by the rotation of the ⟨111⟩ crowdion in the NPC are the main rate limiting processes of the unfaulting mechanism. The effective activation barrier in the transition from the NPC to the glide ⟨111⟩ configuration was calculated by combining the ABC and kinetic Monte Carlo methods and was further benchmarked against molecular dynamics (MD) simulations. The effective activation barrier was found as 0.82 eV; smaller than its previously reported value of 1.68 eV. The ABC method was confirmed to be more efficient than MD, especially for the defect structure evolution processes associated with high barriers and at low temperatures.

DOI: 10.1103/PhysRevB.81.104102 PACS number(s): 61.80.Az

I. INTRODUCTION

Advanced reactors are being designed for longer lifetimes while operating in extreme conditions of temperature, chemical activity, and irradiation.[1] It is thus required to extend our understanding of materials long-term behavior, particularly the nature of radiation-induced defect structures in microstructural evolution. Defects are produced within displacement cascades during irradiation by high-energy particles, neutrons, ions, and electrons. After the cascade formation, many close interstitial atom and vacancy pairs recombine in very short time ($\sim 10^{-11}$ s). Some remaining point defects further accumulate to form self-interstitial atom (SIA) clusters and vacancy clusters. The interaction and migration of such defects are critical in governing the microstructural evolution, which in turn determines the degradation of the macroscopic properties of the reactor materials.[2–6] Material structural, mechanical, and chemical properties change over long time scales as a result of damage accumulation and damage structure evolution,[7–9] leading to consequences as void swelling, irradiation creep, hardening, and chemical segregation. However, it has been a formidable challenge to deal with and predict irradiated microstructural and microchemical evolution over long time (years) using conventional computational methods at the atomistic scale. In this paper, we introduce a new method demonstrated here on a smaller scale problem, with the potential to address in essence this challenge.

The time scale at which the SIA clusters contribute to microstructure evolution is much shorter than that of vacancy clusters.[2–4] Understanding the unfaulting and migration of SIA clusters is of significant importance for nuclear structural materials. Here, we model, simulate, and interpret the evolution and migration of SIA clusters in bcc Fe because ferritic steels are of relevance in the existing and in the design-phase nuclear reactors. Previous molecular dynamics (MD) studies showed that SIA clusters are likely composed of parallel ⟨111⟩ crowdions and do one-dimensional (1D) gliding migration with a very low activation barrier.[10–14] The observations of $\frac{1}{2}\times\langle 111\rangle$ SIA loops' 1D movement in bcc Fe by transmission electron microscopy experiments support the MD predictions of this process qualitatively.[15] However, the resistivity recovery experiments in irradiated bcc Fe upon small-dose irradiation suggested that the activation barriers for small SIA clusters are much higher than the MD prediction.[16,17] This discrepancy indicates that, even for the small SIA clusters, some stable and nonparallel structures might be formed, which could impact the materials' microstructural evolution. The behavior of the small nonparallel SIA clusters could serve as the unit initiation process for the migration and evolution of larger size defects, especially those associated with slow dynamics. However, these stable structures have not been thoroughly probed until only recently. In this context, Terentyev *et al.*[18] proposed the nonparallel configurations (NPC) of small SIA clusters (two-, three-, and four-SIA clusters) as candidates of stable SIA structures. The authors studied these NPC SIA clusters by density-functional-theory calculations and MD simulations with a recent embedded atom method (EAM) potential developed by Ackland, Mendelev, and Srolovitz (AMS).[19] Their results proved that the NPC structures are much more stable than the parallel ⟨111⟩ crowdions. Furthermore, by fitting the Arrhenius relation between temperature and the lifetime of the NPC SIA clusters as found from MD simulations, they calculated the effective activation barrier for the evolution from NPC SIA cluster state to the glide ⟨111⟩ for the two-, three-, and four-SIA clusters. The result for the two-SIA cluster was 0.43 ± 0.08 eV, which was consistent with the value 0.42 ± 0.03 eV given by resistivity recovery experiment[16,17] and by *ab initio* calculations.[20,21] The effective barrier for the unfaulting of the four-SIA cluster was reported to be much higher, 1.68 ± 0.29 eV. However, the details of the unfaulting mechanism and the corresponding evolution in energy for NPC SIA clusters were not provided.

That is because an MD simulation cannot provide easily the complete picture of the energy landscape associated with each possible atomic configuration in the long time scale evolution of an SIA structure. On the other hand, a comprehensive understanding of the potential energy landscape can help elucidate the system's atomic structure evolution and the corresponding kinetics. Many dynamic reactions, including the defect structure evolution, are strongly influenced by the underlying energy landscape of the system's inherent structural configuration.[22] Therefore a challenging problem is whether the energy landscape associated with atomic trajectories can be explored with detail and whether quantitatively reliable results, particularly the effective energy barriers and time scales governing the structural evolution can be derived based on the energy landscape. That is what we address in this paper with a new method, using an SIA cluster from Terentyev *et al.*'s work as a benchmark case.

II. SIMULATION APPROACH

A. Potential energy landscape and atomic trajectories

In this paper, the energy landscape for the evolution of NPC SIA clusters from a trapped state to the glide ⟨111⟩ was identified by the autonomous basin climbing (ABC) method. The ABC method is a new algorithm based on the activation-relaxation methods and explores and reconstructs the system's potential energy surface. It was developed recently by Kushima *et al.*[23,24] in computing the viscosity of supercooled liquids and is based on the Laio and Parrinello's[25] idea of escaping from free-energy minima. Laio and Parrinello's method adds penalty functions to the free energy of a set of collective coordinates in an N-particle system in order to force the system evolve toward rare-event configurations and in doing so, it requires a knowledge of possible reaction coordinates based on input from coarse-grained molecular dynamics. On the other hand, ABC adds penalty functions to the potential energy of the entire $3N$-dimensional space with no prior assumption of the reaction coordinates and with no need to acquire a set of forces from local MD simulations. Therefore, ABC method can serve extremely useful in finding the reaction paths and low-probability configurations without knowing the reaction paths or final configurations in advance. In ABC algorithm, a local minimum-energy state, i, with energy E_i and configuration $\{r_i\}$ is selected at the beginning [Fig. 1(a): (1)]. A series of penalty function additions and total relaxations are then operated in order to make the system climb out of the local basin and reach the next basin [Fig. 1(a): (2)–(4)]. While climbing up a potential hill [steps (1)–(3) in Fig. 1(b)], the total energy (indicated by squares) is always larger than the original potential energy (indicated by circles). When the total energy reaches above a saddle-point energy, upon relaxation a sudden drop in the total energy takes place. This drop corresponds to a new minimum-energy configuration that the system relaxes down to. Therefore, the total energy and the original potential energy at this point are equal [step (4) in Fig. 1(b)]. The crosses represent the highest potential energy that the system reached during that last step. Then, the saddle point, shown by the triangles in Fig. 1(b), and the barrier between the neighboring minima, shown as E_{ij} and E_{ji} in Fig. 1(b), are derived by tracing back the trajectories that the system underwent.

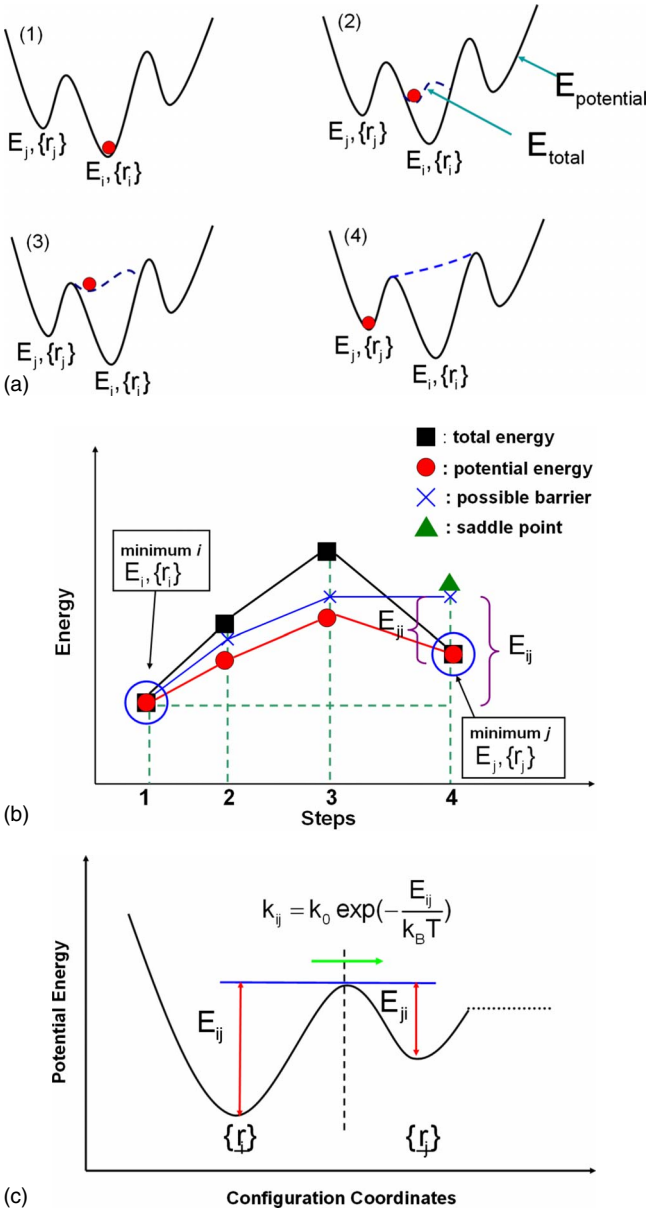

FIG. 1. (Color online) (a) Schematic illustration of the ABC method [figure adapted from (Ref. 23)]. The system climbs out of a potential energy basin (1–3) by adding Gaussian penalty functions to the system's potential energy. Finally, the system reaches the neighboring minimum (4). (b) Trajectory of energy values (1–4) involved in the ABC method, corresponding to the case in (a). (c) Potential energy landscape derived from (b) and the KMC simulation parameters based on it.

While presented in detail by Kushima *et al.*,[23,24] here we summarize the key steps in the ABC algorithm: (a) select an initial local minimum-energy configuration $\underline{r}_1^0$ with energy E_1. The superscript "zero" represents that the configuration corresponds to a minimum. (b) Activation step—add a penalty function of Gaussian form, $\phi_1(\underline{r}) = W \exp[-\frac{(\underline{r}-\underline{r}_1^0)^2}{2\Omega^2}]$, to activate the system out of the minimum-energy configuration. W and Ω are prescribed constants which determine the

strength and spatial extent of the penalty function, respectively. The total system energy now becomes $\Phi_p^1=\Phi+\phi_1$, where Φ_p^1 and Φ represent the total energy and potential energy of the system, respectively. (c) Relaxation step—relax the configuration and energy starting from that at Φ_p^1 to obtain the new energy and configuration $\underline{r}_2$. (d) Repeat steps (b) and (c) with $\Phi_p^2=\Phi_p^1+\phi_2$, $\Phi_p^3=\Phi_p^2+\phi_3,\ldots$, until a relaxation step, n, takes the system to a significantly lower energy state E_2 with configuration $\underline{r}_2^0$. (e) Confirm the sampling of the new local minimum-energy configuration $\underline{r}_2^0$ with energy E_2 by the criterion $\Phi_p^n(\underline{r}_2^0)=\Phi(\underline{r}_2^0)$. This means that the total energy equals to the potential energy at $\underline{r}_2^0$ as the new local minimum. (f) Repeat the operations (a)–(e) above to get a series of minimum-energy configurations in the structural evolution of the system.

By collecting the energy barriers between the different minima, the inherent potential energy landscape of the structure evolution is constructed, as schematically illustrated in Fig. 1(c). Unless the penalty function strength represented by W is too large compared to the energy barrier between the two minima, varying the values of W and Ω should give the same path of evolution between the energy minima. The uniqueness of the reaction path found by the ABC method using an appropriate set of values for W and Ω was illustrated for atomic diffusion on a metal surface by Kushima *et al.*[23] The smaller the penalty function strength, the more accurate the barriers derived in this algorithm are. However, the computational expense also grows with smaller magnitude of the penalty function. In this paper, W and Ω were chosen as 0.25 eV and 0.5 Å^2, respectively, in order to keep a balance between accuracy and computational efficiency.

B. Effective activation barrier and evolution time

Based on the energy landscape found for the evolution of the SIA clusters, the barriers between the different minimum-energy configurations served as input parameters to a kinetic Monte Carlo (KMC) simulation. KMC simulations were set up based on the transition state theory, as schematically shown in Fig. 1(c), and were performed on the lattice. The minimum-energy configurations and the barriers between those configurations for this on-lattice KMC were directly provided by the results from the ABC method, without any assumptions or parameterization involved. The effective migration barrier and the evolution time between the initial state and final state were then calculated by the KMC simulations. KMC simulations also require the values for the pre-exponential coefficients as jump frequencies for each transition between a pair of minimum-energy configurations, denoted as k_0 in Fig. 1(c). The pre-exponential factors are often in the range of 10^{12}–10^{13} s^{-1} (Ref. 26) and in this paper they were chosen to be constant with a value of 5×10^{12} s^{-1} for each of the transitions to a first-order approximation. If all the transitions are associated with a very similar or same value of k_0, then the value of k_0 can only affect the absolute value of the evolution time and not the effective barrier. The latter is the focus in this work; therefore a parameterization or fitting of k_0 was not conducted here.

It is worth reminding here that the static potential energy landscape calculations involved in the current form of the ABC algorithm bare no information on the entropy contribution to the energy. The structure of the algorithm does not prohibit to include the entropy contributions in future development, provided the degeneracy of configurations of saddle points and minima. On the other hand, the entropy is not a significant contributor to the energy barriers in such cases as when the temperature is low or when the potential energy difference is very large. Those cases are of particular importance to slow dynamics in the evolution of trapped structures, as in radiation damage at relatively lower temperatures. In such cases, the KMC simulations based only on the potential energy surface could enable sufficiently good estimate of the energy barriers.

The effective migration barrier calculated by the ABC and KMC methods was then benchmarked against MD simulations of the same type of NPC SIA clusters. The supercell for the MD simulation was cubic with $10a_0\times10a_0\times10a_0$ dimensions and containing 2000 Fe atoms. Interstitial atoms were inserted into the supercell according to the NPC structure proposed by Terentyev *et al.*[18] For comparison purposes, two types of EAM potentials were used in this paper: the AMS potential,[19] the same one as Terentyev *et al.* used, and the Finnis-Sinclair (FS) potential,[27] another well-known EAM potential. To enable statistically sufficient number of MD tests under each temperature, we considered the following criterion, resulting in Eq. (3) below. The microstructural evolution of SIA clusters is a state transition process. According to the transition state theory, the probability distribution function, $p(t)$, for the time, t, of first escape from one energy basin is

$$p(t)=k\exp(-kt), \tag{1}$$

where k is the total jump frequency to neighboring minima.

The average time that the system stays in the given energy basin is the mean lifetime, $\bar{t}$, of the configuration in the basin and is given by

$$\bar{t}=\int_0^\infty k\exp(-kt)t\,dt=\frac{1}{k}. \tag{2}$$

The standard deviation, σ, of the lifetime is then derived as

$$\sigma=\sqrt{\sigma^2}=\left[\int_0^\infty k\exp(-kt)(t-\bar{t})^2dt\right]^{1/2}=\sqrt{\frac{1}{k^2}}=\frac{1}{k}. \tag{3}$$

Theoretically, this result implies that the mean value of the lifetime, $\bar{t}$, should be exactly the same as its standard deviation, σ. Therefore, the number of MD tests should be sufficiently numerous when the calculated average lifetime converges to a value close to its standard deviation. In this paper, 10 MD tests for a given configuration were conducted under each temperature with the AMS potential, 20 MD tests for the FS potential, and both cases satisfied this criterion.

III. RESULTS AND DISCUSSION

A. Unfaulting mechanism of the four-SIA cluster

The four-SIA NPC structure described by Terentyev *et al.*[18] was selected as the starting point in the simulations.

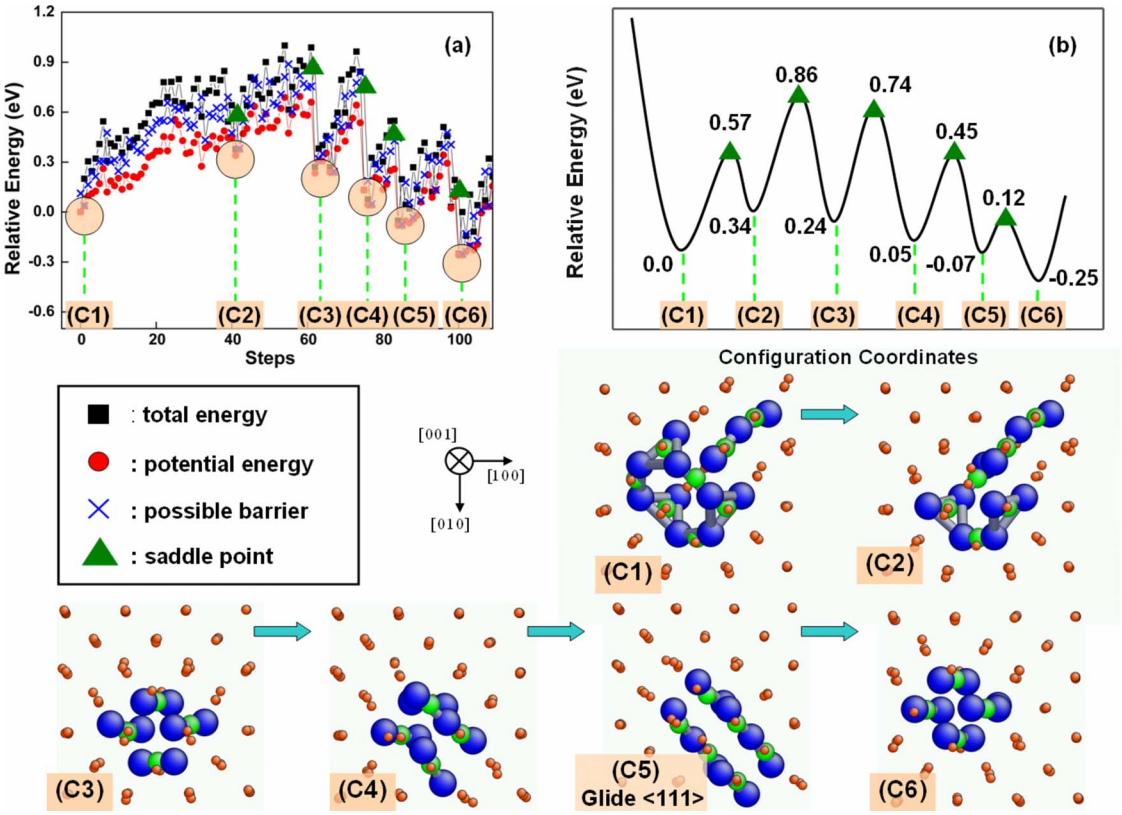

FIG. 2. (Color online) (a) The evolution of energy and atomic trajectories (C1–C6) starting with the initial NPC four-SIA cluster, found by using the ABC method with the AMS potential [visualized by Atomeye (Ref. 28)]. Blue/dark balls represent the interstitial atoms, green/light balls represent the vacant lattice sites, and orange/small balls represent the atoms on lattices. The rods are placed only to accentuate the defect structure but do not represent a physical meaning for a special set of bonds. (b) The potential energy landscape associated with the atomic configurations described in (a).

After relaxation the initial configuration, C1 in Fig. 2, consists of 12 interstitial atoms and eight empty-lattice sites, which gives a net number of four interstitials. Among these, three interstitial atoms and two lattice sites form the ⟨111⟩ crowdion while the remaining nine interstitial atoms and six lattice sites form a ring structure of three trimers on (111) planes. The evolution trajectory and the corresponding energy landscape as derived by the ABC method with the AMS potential is shown in Fig. 2. After being activated by the energy penalty function, the next minimum-energy configuration is C2. In C2, the ⟨111⟩ crowdion remained unchanged while the ring structure of three trimers was broken up due to the returning of the interstitials in one of the trimers back to the nearest vacant lattice sites. Upon further activation, C3 was found as the ⟨111⟩ crowdion rotated to a ⟨110⟩ dumbbell, and consists of three parallel ⟨110⟩ dumbbells and another ⟨110⟩ dumbbell perpendicular to the other three. Then, two ⟨110⟩ dumbbells in C3 rotated to ⟨111⟩ direction. Therefore, C4 consists of two parallel ⟨110⟩ dumbbells and two parallel ⟨111⟩ dumbbells. Evolution of C4 to C5 involved the two ⟨110⟩ dumbbells rotating to the ⟨111⟩ direction, ending up together as the glide ⟨111⟩ configuration. Finally, C6, which consists of four parallel ⟨110⟩ dumbbells, is the lowest-energy structure of the four-SIA cluster. These two last states, C5 and C6, found in this transition are qualitatively consistent with Terentyev *et al.*'s results. Furthermore, the ABC method in our investigation enabled us to identify a detailed set of transition state configurations in the unfaulting process from the trapped to the mobile glide ⟨111⟩ and the associated energy landscape (Fig. 2) at the atomic level. In this process, the transitions C1→C2, C2→C3, and C3→C4 have similar activation barriers, 0.57, 0.52, and 0.50 eV, respectively, that are higher than the other two remaining transitions in the unfaulting. Therefore, based on the activation barriers, the breaking of the initial ring structure of three trimers in (111) planes followed by the rotation of the ⟨111⟩ crowdion are the rate limiting processes of the unfaulting mechanism.

B. Lifetime and effective activation barrier in the unfaulting of the four-SIA cluster

The effective activation barrier in the transition from four-SIA NPC to glide ⟨111⟩ configuration was obtained by the KMC simulations based on the energy landscape produced above by ABC method. In the KMC simulations, the system was initially set at configuration C1 made of the nonparallel SIA cluster shown in Fig. 2 and the simulation was terminated when the system reached C5, the glide ⟨111⟩ configuration. 10 000 KMC simulations were performed under each temperature. Figure 3(a) shows a clear Arrhenius relation between the unfaulting time and temperature with a slope of

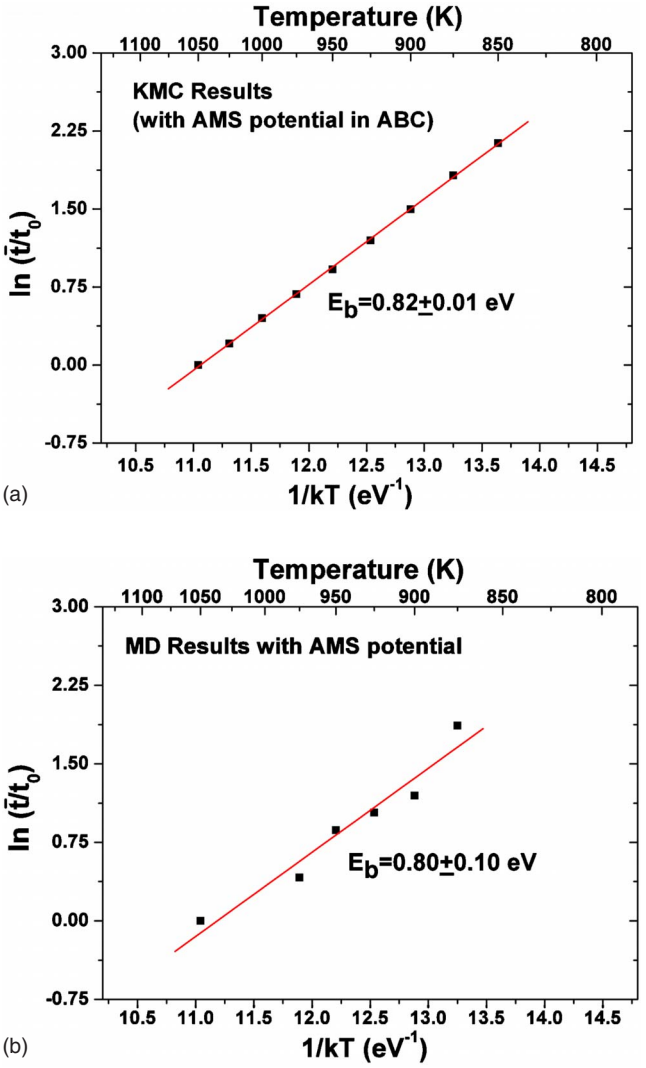

FIG. 3. (Color online) Arrhenius relation between the mean lifetime, $\bar{t}$, of NPC four-SIA cluster and temperature, T (the lifetime at 1050K was set as t_0), with an effective energy barrier of E_b, (a) found by the KMC simulations based on the potential energy landscape generated by the ABC using the AMS potential and (b) found by the MD simulations using the AMS potential.

0.82 ± 0.01 eV, which gives the effective activation barrier. The advantage here is that the configurations and the corresponding energy barriers in KMC are not presumed but rather precisely described by the results from the ABC method. While here we are investigating a relatively small defect structure for benchmarking the method, this approach would be particularly important for accuracy when multiple defect configurations may interact as a function of their size, structure, and separation distance or if complicated defect interactions yield unexpected new configurations. In those cases, the interaction paths and barriers could no longer be assumed to be constant under different local environments, as is typically the limiting presumption in conventional KMC methods.

Compared with the migration barrier for the glide ⟨111⟩ movement (tens of millielectron volt[10–12]), this value of 0.82 eV corresponds to a very high activation energy for the unfaulting of the NPC four-SIA cluster. This means that the configuration C1 is a rather stable structure, consistent qualitatively with Terentyev *et al.*'s conclusion. In our investigation, the effective activation barrier calculated from the ABC and KMC simulations was benchmarked against MD tests using the same EAM potential. Configurations C2 and C3 were also found in the MD simulations, which are consistent with the evolution trajectory given by the ABC method. C4 was seldom found in the MD simulations at these rather high temperatures because the barrier between C4 and C5 is relatively low. The quantitative results for the unfaulting time taken from the MD results are shown in Table I.

TABLE I. The mean and the standard deviation of the lifetime in the unfaulting of the NPC four-SIA cluster found from the MD simulations using the AMS potential.

Temperature (K)	Mean lifetime, $\bar{t}$ (ps)	Standard deviation, σ (ps)
1050	18.65	30.08
975	28.20	34.09
950	44.44	39.78
925	52.50	54.25
900	61.72	49.16
875	120.47	99.07

As seen in Table I, the calculated mean lifetime and its standard deviation are sufficiently close to each other. This implies statistical reliability of the MD-driven results, based on the criterion described by Eqs. (2) and (3). Using the mean lifetime versus temperature data, which obeys the Arrhenius behavior as shown in Fig. 3(b), the effective activation energy in transition from NPC cluster to glide ⟨111⟩ cluster with the MD benchmark tests is 0.80 ± 0.10 eV.

The evolution of the NPC four-SIA cluster by the ABC method using the FS potential was also studied here. The energy landscape was slightly different from the one given by the AMS potential [Fig. 2(b)]. Nevertheless, the NPC structure is still a stable one and the KMC calculations resulted in 1.032 ± 0.002 eV (rounded to 1.03 eV) for the effective migration barrier between the NPC structure and glide ⟨111⟩ configuration. 20 MD benchmark tests with the FS potential were conducted under each temperature for validating the ABC and KMC results. The effective migration barrier of 1.09 ± 0.16 eV was found by fitting the lifetime of NPC cluster, similarly as in Fig. 3(b) for the AMS potential.

The MD results of 0.80 and 1.09 eV with the AMS and the FS potential, respectively, are clearly consistent with the 0.82 and 1.03 eV effective barriers calculated by the ABC and KMC simulations in this work. As noted in the simulation approach, the KMC results based on the ABC-driven energy barriers here do not include entropy contributions. The reason that they are well consistent with the MD-driven energy barriers could be that the entropy difference between the initial point, C1, and the main saddle point located between C2 and C3 determining the barrier for the unfaulting process is very small compared to the potential energy difference between them. The consistent benchmarking of the results with the MD tests proves that the ABC method is

quantitatively capable of capturing the transitions in the atomic structure of the SIA clusters and the corresponding energy landscape.

On the other hand, these values are significantly different from the 1.68 eV given by Terentyev *et al.*'s MD results using the same AMS potential. According to the criteria we described in Eqs. (2) and (3), the MD results for estimating the lifetime in this transition states context can be statistically acceptable only when the standard deviation is close to the calculated mean lifetime. However, only one MD result data point was provided for the lifetime at the relatively low temperature around 800 K by Terentyev *et al.*[18] Therefore, the mean and the standard deviation of the lifetime calculated in Ref. 18 for the four-NPC SIA cluster around 800 K is not clear quantitatively. Such a low number of MD runs at the given temperature could be the cause for the loss in accuracy of the unfaulting energy barrier result reported by Terentyev *et al.* for the NPC four-SIA cluster.

The last point worth mentioning here is the time savings with the ABC simulations when compared with MD and we give an example for this comparison. In this paper, the mean lifetime of the NPC cluster is about 100 ps in the temperature range of ~800 K–1000 K. It takes 10^5 steps for a single MD test with a time step of 10^{-15} s to capture the transition with this lifetime. Furthermore, considering several temperatures and approximately 10–20 MD tests at each temperature for achieving statistically reliable results, the total time steps consumed in the MD simulations amount to about 10^7. On the other hand, with the ABC method, only several hundred simulation steps are sufficient for a typical transition trajectory [Fig. 2(a)]. Although a step in ABC method is longer than in MD (about 10^3 times longer), the total simulation time consumed by the ABC simulations is considerably less. In this case of study, ABC method is more than ten times faster than the MD simulation. This advantage is expected to be more significant for processes associated with slow dynamics—that is with very high transition energy barriers and at relatively lower temperatures.

IV. CONCLUSIONS

In this study, we reported on the structural evolution of a trapped self-interstitial atom cluster in bcc Fe, capturing the atomic scale transitions, the corresponding potential energy landscape and the unfaulting time scale. The potential energy landscape in the unfaulting from the trapped to the mobile glide ⟨111⟩ configuration was explored by tracing the atomic trajectories in detail, using the ABC method. The breaking of the initial ring structure of three trimers on (111) planes followed by the rotation of the ⟨111⟩ crowdion are the rate limiting processes of the unfaulting mechanism. The minimum and saddle-point energies in all the transitions were specifically quantified. The effective activation barrier for the entire unfaulting process was calculated by combining the ABC and KMC methods, and was also benchmarked against MD simulations. The results from the two approaches showed good consistency.

An effective barrier of 0.82 eV was found for the unfaulting of the NPC four-SIA cluster modeled by the ABC and KMC methods, and is significantly different from the previously published result.[18] However, the consistent benchmarking of this result with the MD tests in this work indicates that this barrier is rational and proves that the ABC method is capable of capturing the transitions in the atomic structure of the SIA clusters and the corresponding energy landscape. Therefore, we introduce the ABC method as a new algorithm based on the activation-relaxation methods to effectively capture the atomistic scale details of the slow dynamics involved in the evolution and migration of interstitial defects in irradiated materials. While the unfaulting process in this paper spans over a rather short time scale for a small system, the principles for the ABC method in the evolution of irradiation induced defects with atomic structure relaxations shown here apply for any size and time scale in materials behavior. As noted in the Introduction, a particularly long time scale process, slow dynamics in glass transition, with relaxation time scales up to 10^9 s has been already successfully modeled by Kushima *et al.*[23,24] with the ABC method. This time scale is on the order of the operation time of nuclear reactors. The demonstration on the atomic defect structures in bcc Fe in this work and Kushima *et al.*'s glass transition study together suggest that the simulation method development based on the ABC principles can be particularly useful in predicting how the macroscopic mechanical and chemical properties change in an irradiated material while retaining atomistic fundamentals—this is the ultimate challenge in simulating long time scale behavior upon radiation damage in nuclear materials.

ACKNOWLEDGMENTS

We gratefully acknowledge S. Yip and P. Monasterio for precious suggestions, discussions, and feedback.

*Corresponding author; byildiz@mit.edu

[1] R. W. Grimes, R. J. M. Konings, and L. Edwards, Nature Mater. **7**, 683 (2008).
[2] L. K. Mansur, J. Nucl. Mater. **216**, 97 (1994).
[3] L. K. Mansur, in *Kinetics of Nonhomogeneous Processes*, edited by G. R. Freeman (Wiley, New York, 1987), pp. 377–463.
[4] L. K. Mansur, Nucl. Technol. **40**, 5 (1978).
[5] G. S. Was, J. Nucl. Mater. **367-370**, 11 (2007).
[6] G. R. Odette, M. J. Alinger, and B. D. Wirth, Annu. Rev. Mater. Res. **38**, 471 (2008).
[7] D. S. Gelles, J. Nucl. Mater. **225**, 163 (1995).
[8] Y. Katoh, A. Kohyama, and D. S. Gelles, J. Nucl. Mater. **225**, 154 (1995).
[9] Yu. V. Konobeev, A. M. Dvoriashin, S. I. Porollo, and F. A. Garner, J. Nucl. Mater. **355**, 124 (2006).
[10] B. D. Wirth, G. R. Odette, D. Maroudas, and G. E. Lucas, J.

Nucl. Mater. **244**, 185 (1997).
[11] N. Soneda and T. D. Rubia, Philos. Mag. A **81**, 331 (2001).
[12] Yu. N. Osetsky, D. J. Bacon, A. Serra, B. N. Singh, and S. I. Golubov, Philos. Mag. **83**, 61 (2003).
[13] J. Marian, B. D. Wirth, A. Caro, B. Sadigh, G. R. Odette, J. M. Perlado, and T. Diaz de la Rubia, Phys. Rev. B **65**, 144102 (2002).
[14] A. Takahashi and N. M. Ghoniem, Phys. Rev. B **80**, 174104 (2009).
[15] K. Arakawa, M. Hatanaka, E. Kuramoto, K. Ono, and H. Mori, Phys. Rev. Lett. **96**, 125506 (2006).
[16] C. C. Fu, J. D. Torre, F. Willaime, J. L. Bocquet, and A. Barbu, Nature Mater. **4**, 68 (2005).
[17] S. Takaki, J. Fuss, H. Kugler, U. Dedek, and H. Schultz, Radiat. Eff. **79**, 87 (1983).
[18] D. A. Terentyev, T. P. C. Klaver, P. Olsson, M. C. Marinica, F. Willaime, C. Domain, and L. Malerba, Phys. Rev. Lett. **100**, 145503 (2008).
[19] G. J. Ackland, M. I. Mendelev, D. J. Srolovitz, S. Han, and A. V. Barashev, J. Phys.: Condens. Matter **16**, S2629 (2004).
[20] C. Domain and C. S. Becquart, Phys. Rev. B **65**, 024103 (2001).
[21] C. C. Fu, F. Willaime, and P. Ordejon, Phys. Rev. Lett. **92**, 175503 (2004).
[22] S. Sastry, P. G. Debenedetti, and F. H. Stillinger, Nature (London) **393**, 554 (1998).
[23] A. Kushima, X. Lin, J. Li, J. Eapen, J. C. Mauro, X. F. Qian, P. Diep, and S. Yip, J. Chem. Phys. **130**, 224504 (2009).
[24] A. Kushima, X. Lin, J. Li, X. F. Qian, J. Eapen, J. C. Mauro, P. Diep, and S. Yip, J. Chem. Phys. **131**, 164505 (2009).
[25] A. Laio and M. Parrinello, Proc. Natl. Acad. Sci. U.S.A. **99**, 12562 (2002).
[26] A. F. Voter, in *Radiation Effects in Solids*, NATO Science Series II: Mathematics, Physics and Chemistry, edited by K. E. Sickafus, E. A. Kotomin, and B. P. Uberuaga (Springer, Dordrecht, The Netherlands, 2006), pp. 1–24.
[27] M. W. Finnis and J. E. Sinclair, Philos. Mag. A **50**, 45 (1984).
[28] J. Li, Modell. Simul. Mater. Sci. Eng. **11**, 173 (2003).